Sulfur reduction coupling with anaerobic ammonium oxidation power the origin of life

Peng Bao[1, 2, *], Guo-Xiang Li[1, 2, 3], Hu Li[1]

[1]Key Lab of Urban Environment and Health, Institute of Urban Environment, Chinese Academy of Sciences, Xiamen 361021, P. R. China

[2]Ningbo Urban Environment Observation and Station, Chinese Academy of Sciences, Ningbo 315800, P. R. China

[3]University of Chinese Academy of Sciences, Beijing 100049, P. R. China

Address correspondence to:

Dr. Peng Bao

Institute of Urban Environment, Chinese Academy of Sciences, Xiamen 361021, P. R. China

E-mail: pbao@iue.ac.cn; neilbao17@163.com

Abstract

The geochemical energy that drives the transition from non-life to life is as yet unknown. We found that sulfurous species reduction coupling with anaerobic ammonium oxidation (Sammox), could provide the primordial redox equivalents and energy for the reductive acetyl-CoA pathway combined with incomplete reductive tricarboxylic acid (rTCA) cycle and reductive amination. Fe-S mineral/metal alloy catalysis and thiols/thioesters as energy couplers could enhance the efficiency of Sammox-powered proto-anabolic networks. Genomic analysis of Sammox bacterium *Ralstonia thioammoniphilus* GX3-BWBA implied that this ancient metabolism in modern microbes should contain two stages according to ammonium transformation, —oxidation of ammonium to nitrite and denitrification. The incomplete rTCA cycle and reductive acetyl-CoA pathway were all identified in *R. thioammoniphilus* metabolic networks, which were responsible for chemolithotrophic metabolism. Sammox drove the coupling of the biochemical transformation of C, H, O, N, S, and/or Fe simultaneously in Hadean alkaline hydrothermal systems, thereby permitting the emergence of life. The results bridged the gap in the transition from geochemistry to biochemistry.

Introduction

The transition from non-life to life occurred in the context of geochemical energy derived from element-coupled transformation[1-3]. The chemistry of life is based on redox reactions, that is, successive transfers of electrons and protons from the six major elements, i.e., C, H, O, N, S, and P[1,4]. The H_2/CO_2 redox couple, which can occur in submarine hydrothermal vents, has been proposed to drive the reductive acetyl-CoA pathway, an ancient metabolic route[3,5-7]. Nevertheless, the primordial energy source of the H_2/CO_2 redox couple suffers from the difficulty that the exergonic reaction competes with the endergonic reaction for available H_2[8]. The subsequent surface metabolism and thioester world theories still could not answer the question, how the required reduced carbon compounds have been synthesized[9,10]. Despite this limitation, these theories have emphasized the important roles of thioesters and Fe-S mineral catalysis for driving the primordial rTCA cycle, a central anabolic biochemical pathway whose origins are proposed to trace back to geochemistry[9,11,12].

Native iron/metals were recently shown to promote the reductive acetyl-CoA pathway and rTCA cycle and strongly support the feasibility of these two primordial synthetic pathways[13,14], although they were generally considered to be rare near the Earth's surface[13] and cannot support the long elemental transition from geochemistry to biochemistry. Proto-anabolic networks consisting of the reductive acetyl-CoA pathway together with the complete/incomplete rTCA cycle as primordial synthetic pathways are therefore more logical[3,15-18]. However, the initial driving force for the rise of proto-anabolic networks is still unclear. Moreover, the roles of N and S

geochemical transformation in the origin of life have been largely ignored because computational analysis has implied that N and S are essential for thermodynamically feasible phosphate-independent metabolism before the rise of last universal common ancestor (LUCA)[19]. The proto-anabolic networks would necessarily be driven by C, H, O, N, S, and/or Fe coupling transformation at their earliest stage of the transition from geochemistry to biochemistry. The co-evolution of the metabolism of those elements may provide strong explanatory power for the origin of life and explain why the structure of metabolic networks is as it is. We therefore speculate that thermodynamically feasible sulfurous species reduction coupling with anaerobic ammonium oxidation reaction[20,21] (Eqs. 1, 2), with/without the catalysis of Fe-S minerals and thioesters, may have been the primordial power force for the rise of proto-anabolic networks.

$$8NH_4^+ + 2SO_4^{2-} + 2HCO_3^- \rightarrow 4N_2 + 2HS^- + CH_3COO^- + 12H_2O + 5H^+ \quad \Delta G_r = -20.0 \text{ kJ mol}^{-1} \quad (1)$$

$$4NH_4^+ + S_2O_3^{2-} + 2HCO_3^- \rightarrow 2N_2 + 2HS^- + 2HCOO^- + 5H_2O + 4H^+ \quad \Delta G_r = -13.4 \text{ kJ mol}^{-1} \quad (2)$$

On early Earth, elemental sulfur, sulfite, and thiosulfate were produced abundantly from volcanic and hydrothermal SO_2 or from H_2S oxidation by iron oxides in sulfide-rich hydrothermal fluid[2,15,22]. In simulated hydrothermal systems with conditions of 300 °C and high pressure, nitrite was readily converted to NH_3[23], and Ni-Fe metals and alloys were also effective catalysts of N_2 reduction to NH_3 in Hadean hydrothermal systems[24]. There would have been much higher CO_2 concentrations in the oceans on early Earth because there was perhaps up to 1000 times more CO_2 in the atmosphere than that today[25].

Hence, when sulfurous species and NH_3 in Hadean hydrothermal systems made contact with CO_2, there were spontaneous electron and proton transfers for energy generation and organic molecule synthesis via sulfurous species reduction coupling with ammonium oxidation. We termed this process Sammox, which falls outside of previous studies of the coupling elemental biogeochemical cycles[1,26]. A prebiotic reaction should occur with the ability to branch out into S and N biochemistry, which could contribute to the autocatalysis and evolution of primordial metabolic networks. Thus, Sammox may facilitate the synthesis of thioesters and amino acids, which are essential for the self-amplification of phosphate-independent metabolic networks before the rise of LUCA. We expect that prebiotic chemical evidence of Sammox-powered CO_2 fixation, thioesters, and amino acid synthesis, combined with genetic analysis of a representative Sammox microbe, will provide profound insights into the earliest origins of life and fill in the missing link of the emergence of biochemistry from geochemistry.

Sammox and the construction of proto-anabolic networks

We set out to verify the feasibility of Sammox-driven prebiotic reductive acetyl-CoA pathway, rTCA cycle, and reductive amination and to determine how methanethiol and Fe-S mineral catalysis enhance the reactions in both thiosulfate- and sulfate-fueled Sammox systems. Formate and acetate were the products of Sammox-driven reductive acetyl-CoA pathway (Fig. 1). We haven’t detected pyruvate as the end-product of Sammox-driven reductive acetyl-CoA pathway because

pyruvate quickly entered the incomplete rTCA cycle as a reaction substrate (Figs. 2, 3). We qualitatively identified methyl acetate as a product in Sammox reaction systems (Extended Data Fig. 1), implying that methanol should be an intermediate of Sammox-driven reductive acetyl-CoA pathway (Fig. 3a). More importantly, this result confirmed the capacity for Sammox-powered ester bond formation, which was critical for the synthesis of complex organic molecules, such as lipids and RNA[27].

We quantitatively identified succinate and α-ketoglutarate, and qualitatively identified polypyrrole (data not shown) and glutamate as products of Sammox-driven incomplete rTCA cycle (Figs. 1, 2, Extended Data Fig. 2). Glutamate came from the reductive amination of α-ketoglutarate with ammonium, while the existence of polypyrrole implied that there should be pyrrole derived from succinate. This provided the possibility of biocatalysis. We haven't detected other intermediates of the incomplete rTCA cycle, potentially because of their low productivity. There were no side reactions of pyruvate to lactate or α-ketoglutarate to α-hydroxyglutarate[16], which allowed Sammox-driven proto-anabolic networks to persist and self-amplify.

Sulfate-fueled Sammox was more effective than thiosulfate-fueled Sammox (Figs. 1, 2), due to the higher energy yield of the former reaction (Eqs. 1, 2). Both Fe-S minerals and methanethiol could enhance the efficiency of the thiosulfate-fueled Sammox reaction but not the sulfate-fueled Sammox reaction (Fig 1), logically implying that the thiosulfate-fueled Sammox reaction should be the primordial reaction driving the construction of proto-anabolic networks. Note that methanethiol was more effective than Fe-S minerals for promoting the thiosulfate-fueled Sammox

reaction (Fig. 1a). It incorporates into C, H, O and N biochemical transformation via thiol-thioester exchange[9], transforming itself and other organic reaction products into new organic products[10], therefore resulted in the coupling biochemical transformation of C, H, O, N, and S and the expansion of primordial metabolic networks. We deduced that when reaction conditions were met in Hadean hydrothermal systems, Sammox-generated proton gradient could modulate reduction potential similar to applying a voltage, leading to electrocatalytic CO_2 reduction with/without catalysis of Fe-S minerals and thioesters[28,29]. Thus, almost all of the essential metabolic precursors for biosynthesis could be provided in one geological setting. The organics formed within the vent pores in Hadean hydrothermal systems, where they should concentrate via processes, such as thermophoresis, and potentially form structures, such as lipid membranes lining hydrophobic walls[7,15,30]. Thereby, Sammox gave rise to the origin of not free-living organic precursor on the surface of Fe-S minerals[31] (Fig. 3c).

As one of the products of Sammox, sulfide began to increase in the Hadean oceans, facilitating thiols synthesis on Fe-S mineral surface[28] and leading to de Duve's thioester world and the boom of S biochemistry. As a result, the S isotope geochemical evidence can be traced back to 3.8 Ga and has been well preserved[4,22,32,33]. Biogenic sulfide reacted with soluble Fe^{2+} and/or Ni^{2+}/Co^{2+}/Se to maintain a continuous self-supply of freshly precipitated FeS and/or metals alloys and even subsequent enzyme and redox protein active centers, such as ferredoxin[34]. This may represent a route for S and Fe assimilation, which would facilitate escape of the

not free-living organic precursor from the surface of Fe-S minerals. As catalytic properties improved, the yield of proto-anabolic networks increased, ultimately extending the pathway through to C_6 tricarboxylic acids. Sulfur biogeochemistry stimulated iron redox geochemistry; therefore, ferrous iron was released due to the abiotic reduction of iron oxyhydroxide by biogenic sulfide, thus resulting in phosphite liberation from ferruginous sediments[35]. In this study, we will not discuss how P incorporated into primordial metabolic networks, but infer that Sammox-driven proto-anabolic networks could facilitate self-evolution through optimizing the ambient environment to make it sufficiently stable and habitable for life.

Discovery of Sammox microbe

We successfully isolated a pure Sammox culture (designated GX3-BWBA) that could conserve energy from the reduction of sulfurous species (thiosulfate, sulfate, sulfite, and elemental sulfur) coupled to anaerobic ammonium oxidation. Strain GX3-BWBA appeared as bean-shaped cells with a diameter of 0.6 μm and a length of 1.0 μm and harbored a single flagella with a bacterial capsule (Fig. 4a, b, Extended Data Fig. 3). Comparative sequence analysis of 16S rRNA genes revealed a 99% query cover and 99% sequence identity between strain GX3-BWBA and a series of uncultured *Ralstonia* bacterial clones (Fig. 4c). Thus, strain GX3-BWBA was phylogenetically clustered within the *Ralstonia* genus (Fig. 4c). GX3-BWBA grew to a maximal density of 1.6×10^5 CFU ml^{-1} in anaerobic freshwater mineral medium containing bicarbonate, ammonium, and thiosulfate/sulfate as the sole carbon and

energy sources, suggesting chemoautotrophy (Fig. 4b). Approximately 8 μM ammonium was sufficient to support the chemoautotrophic growth of strain GX3-BWBA, demonstrating high affinity for ammonium (data not shown). Thiosulfate was the preferred electron acceptor over sulfate by GX3-BWBA (Fig. 4b). There was no significant growth of GX3-BWBA under conditions without ammonium or sulfurous species (Fig. 4b); thus, ammonium and sulfurous species were essential factors for GX3-BWBA chemoautotrophic growth. We provisionally classified this Sammox bacterium as "*Ralstonia thioammoniphilus*" (thi.o.am.mo.ni' phi.lus. Gr. n. *thion* sulfur; L. neut. n. *sal ammoniacum* salt of Ammon (NH_4Cl); Gr. adj. *phylos* loving; N.L. neut. adj. *thioammoniphilus* sulfur-ammonium-loving).

As a probable ancient chemoautotroph, Sammox microbe preferred other sulfurous species, except for sulfate, potentially because elemental sulfur, thiosulfate, and sulfite were produced abundantly from ancient volcanic and hydrothermal SO_2 or from sulfide oxidation by iron oxides in sulfide-rich hydrothermal fluid[2,15,22]. Thiosulfate constituted 68–78% of the immediate HS^- oxidation products and was involved in a dynamic HS^--$S_2O_3^{2-}$ cycle in anoxic marine and freshwater sediments[36]. In contrast, sulfate would have had only very limited, localized significance[2].

We further tested thiosulfate- and sulfate-fueled Sammox reactions using *R. thioammoniphilus*, and the end product N_2 generation rate was measured (Fig. 4c, d). The generation rate of N_2 in the thiosulfate treatment group was slightly higher than that in the sulfate treatment group (Fig. 4c, d). The production rate of $^{29}N_2$ was about 2.5 nmol ml^{-1} day^{-1}, which was significantly higher than $^{30}N_2$ (approximately 2.5 pmol

ml^{-1} day^{-1}; Fig. 4c, d). Figure 5 shows the coupled dynamic transformation of sulfurous species and ammonium during Sammox process. In thiosulfate-fueled Sammox, sulfide was the product of the thiosulfate reduction, whereas sulfite was an intermediate (Fig. 5a). Ammonium oxidation accompanied by thiosulfate reduction was significant compared with that in the control group. As intermediate of ammonium oxidation, nitrite significantly increased on day 27 (Fig. 5b). Based on the low concentration, we did not determine the dynamic generation of dinitrogen to avoid leakage. There was weak but significant sulfate reduction in the sulfate-fueled Sammox group, accompanied by sulfide generation (Fig. 5c). The concentration of nitrite also showed a slight increase during the ammonium oxidation process (Fig. 5d). The concentrations of sulfurous species and ammonium showed no significant changes in the control group (Fig. 5). The assumed net thiosulfate-/sulfate-fueled Sammox reactions are shown in Eqs. 1 and 2. The generation of precursors of CO_2 fixation was thermodynamically favorable by Sammox.

Notably, quite a few iron oxides could be abiotically reduced by sulfide generated from Sammox in an iron-rich environment, then an illusion of ferric iron reduction coupled to anaerobic ammonium oxidation (Feammox) arises[37-39]. Indeed, it is still unclear to what extent Sammox overlaps with Feammox; however, we can infer that Sammox may be widely distributed in different anoxic environments based on the ubiquity of *Ralstonia* spp. and its high affinity for ammonium. Moreover, as an ancient type of metabolism, there may be a variety of microbes that still preserved this living strategy.

Genomic and N, S, and C metabolic gene analyses

To elucidate the mechanisms of Sammox reaction in modern microorganisms, we sequenced the genome of *R. thioammoniphilus* (Extended Data Table 1, Extended Data Fig. 4). There were denitrification genes in the *R. thioammoniphilus* genome, including copper-containing nitrite reductase (*nirK*), nitric oxide reductase (*norB*), and nitrous oxide reductase (*nosZ*) (Fig. 6a). This result confirmed that nitrite was the expected intermediate product of Sammox and that the thiosulfate-/sulfate-fueled Sammox reactions in *R. thioammoniphilus* contained two stages: oxidation of ammonium to nitrite (Eqs. 3 and 4)[21], followed by the final step of the denitrification pathway which is reduction of nitrite to dinitrogen (Eq. 5).

$$4NH_4^+ + 3S_2O_3^{2-} \rightarrow 4NO_2^- + 6HS^- + H_2O + 8H^+ \quad (3)$$

$$4NH_4^+ + 3SO_4^{2-} \rightarrow 4NO_2^- + 3HS^- + 4H_2O + 5H^+ \quad (4)$$

$$+2NO_2^- + 8H^+ + 6e^- \rightarrow N_2 + 4H_2O \quad (5)$$

We did not find any other anaerobic ammonium oxidation-related functional genes in the genome of *R. thioammoniphilus* (Fig. 6a). Thus, the ammonium oxidation in Sammox was different from that in complete ammonium oxidation (Comammox) and anaerobic ammonium oxidation (Anammox)[26].

Our main concern is how ammonium was oxidized by thiosulfate/sulfate into nitrite. Sammox in *R. thioammoniphilus* may still need an iron-sulfur catalyst that inherited from proto-anabolic networks. As lacking of genetic evidence about Sammox, we predicted that ferredoxin oxidoreductase (e.g., nitrite/sulfite reductase

ferredoxin domain protein and ferredoxin-nitrite reductase) or other iron-sulfur enzymes encoded by genes with unknown sequences may mediate sulfur reduction coupling with ammonium oxidation to nitrite (Eqs. 3–6, Extended Data Schematic 1). Here, thiosulfate should be first transformed into sulfite, which could be reduced by ferredoxin. Hence, Sammox reversed the nitrite reduction process. This process was quite similar to a nitrite generation pathway in Feammox process (Eq. 7)[26,37,38], implying its theoretical feasibility. Electrons and protons generated in the first stage of Sammox reaction were used to drive nitrite reduction to dinitrogen. As a highly exergonic reaction, energy released from nitrite reduction drove CO_2 fixation.

$$NH_4^+ + 6\ \text{oxidized ferredoxin} + 2H_2O \rightarrow NO_2^- + 6\ \text{reduced ferredoxin} + 8H^+ \quad (6)$$

$$NH_4^+ + 6Fe^{3+} + 2H_2O \rightarrow NO_2^- + 6Fe^{2+} + 8H^+ \quad (7)$$

However, so far we do not clearly know the molecular mechanisms of sulfate reduction coupling with ammonium oxidation to nitrite. *R. thioammoniphilus* contains no ATP sulfurylase (Sat)-coding gene (Fig. 6a), suggesting that sulfate reduction in sulfate-fueled Sammox is different from dissimilatory sulfate reduction. Dissimilatory sulfate reduction may be later than sulfate reduction in sulfate-fueled Sammox, according to isotope geochemical evidence[22,40,41]. This is why sulfite reductase (Extended Data Table 2, Extended Data Fig. 5) showed a much more extensive distribution than Sat (Extended Data Table 3, Extended Data Fig. 6) and, also the evidence for ancient metabolic networks led to the emergence of living systems prior to the incorporation of P[19].

As we have inferred that the transition of geochemistry to biochemistry of S and

N should start at the same starting point. Sulfite and nitrite reductases belong to the only class of enzymes that share a common architecture as well as a requirement for a siroheme cofactor[42]. The phylogenetic tree indicated that the putative multifunctional sulfite/nitrite reductase of archaea and eukaryota gathered into one and three clusters, respectively. Putative interdomain lateral gene transfer may result in the distribution of some archaea and eukaryota multifunctional sulfite/nitrite reductases into bacterial clusters (Fig. 6b). Similar to sulfite reductase, nitrite reductase is widely distributed in all types of modern organisms (Extended Data Table 4, Extended Data Fig. 7), and indeed, sulfite reductases from some sources can catalyze the reduction of both sulfite and nitrite[42]. This phenomenon suggested that S and N biochemistry may have a common evolutionary origin derived from Sammox.

Similar to the sulfite/nitrite reductase, some biomolecules as remnants of Sammox and ancient metabolism may be hidden in the architecture of the metabolic networks of *R. thioammoniphilus*. In theory, such "metabolic fossils" for the origin of the coupled transformation of elements should be widely distributed in all types of modern organisms as well. Thiosulfate may be the most preferential electron acceptor for Sammox in Hadean hydrothermal systems, leading to the wide distribution of multifunctional rhodanese (thiosulfate sulfurtransferase) in prokaryotes, eukaryotes, and archaea (Extended Data Table 5, Extended Data Fig. 8). Rhodanese has been proposed to have an assimilatory role using dithiol dihydrolipoate as the sulfur acceptor and acting as a sulfur insertase involved in the formation of prosthetic groups in iron-sulfur proteins, such as ferredoxin[43,44]. This implies that rhodanese may be the

primary mechanism for the formation of the iron-sulfur center of primordial enzymes to catalyze proto-anabolic networks in LUCA, thus indicating its ancient nature. Rhodanese can also catalyze a sulfur dissimilatory metabolic reaction which is thiosulfate cleavage to sulfite[44] (Scheme 1), thereby facilitate thiosulfate involve in the first stage of Sammox.

$$S_2O_3^{2-} + 2R\text{-}S^- \rightarrow SO_3^{2-} + R\text{-}S\text{-}S\text{-}R + S^{2-}$$

Scheme 1

The structural similarity between rhodanese and Cdc25 phosphatases indicated the common evolutionary origin of the two enzyme families[45]; alternatively, phosphatases may originate from the rhodanese family because P incorporation occurred later than S incorporation in metabolic networks. This evidence implied the relationship between S and P metabolic evolution.

Six candidate genes encoding components of the reductive acetyl-CoA pathway were identified as formate dehydrogenase (fdoI), 5,10-methenyl-H4 folate cyclohydrolase (folD), 5,10-methylene-H4 folate dehydrogenase (folD), 5,10-methylene-H4 folate reductase (metF), CO dehydrogenase/acetyl-CoA synthase (acs), and pyruvate:ferredoxin oxidoreductase (PFOR) (Fig. 6a). Three gene homologs 10-formyl-H4 folate synthetase, methyl-H4 folate:corrinoid iron-sulfur protein methyltransferase, and corrinoid iron-sulfur protein appeared to be missing. It is possible that the present genomic analysis was insufficient to distinguish whether *R. thioammoniphilus* could facilitate CO_2 fixation via the incomplete reductive acetyl-CoA pathway or there were functional related enzymes encoded by genes with

unknown sequences[46].

In annotations of the rTCA cycle, two essential gene homologs appeared to be missing (Fig. 6a). One of the missing genes, α-oxoglutarate synthase, catalyzes reductive carboxylation from succinate to α-ketoglutarate, and the other is citryl-CoA synthetase. Two potential reversible ATP-dependent citrate lyase subunits (ACL) (citE, mdcC) were identified (Fig. 6a), which was a key indication for autotrophic CO_2 fixation via the rTCA cycle instead of citrate synthase[47]. These results suggested the potential of *R. thioammoniphilus* for carbon fixation via the incomplete reductive acetyl-CoA pathway and rTCA cycle.

Final remarks: from metabolic innovation to evolution

This finding, Sammox powered the origin of life, provided strong evidence of prebiotic Sammox-driven proto-anabolic networks and a Sammox microbe, *R. thioammoniphilus*. Our study was partially supported by the theory of a chemoautotrophic origin of life supported by surface metabolism and a primordial iron-sulfur world[9,11]. Here, Fe-S minerals and/or metal alloy catalysis enhanced product generation of Sammox rather than providing hydrogen for CO_2 reduction. The Fe-S mineral surfaces, where transition metal ions, such as Ni^{2+}, Co^{2+}, or Se, are catalytically active[48], and also the very place facilitated Sammox-driven amnio acids and thioesters synthesis. Therefore, a mixture of Fe-S minerals and transition metal ions may have been the evolutionary precursor of the enzymatic active center, when chelated by amnio acids, converted to biocatalysts[29,34]. In this regard, our study could

explain the occurrence of enzymes with Fe-S reaction centers in the electron transport chains of most known extant bioenergy flows in all three kingdoms of life. Thioesters derived during Sammox reaction provided the energetic and catalytic framework of Sammox, and feedback and feedforward to Sammox-driven proto-anabolic networks, ultimately leading to metabolic reproduction and innovation[48]. Thus, Sammox drove the emergence of the primordial structure and function of the not free-living organic precursor, a ligand sphere, held together by bonding to the surfaces of Fe-S minerals (Fig. 3c). The feedback coupling between the primordial metabolic networks and their environment could shape the evolution of both[49]. As a self-regulating system, C, H, O, N, S, and/or Fe coupling metabolic networks could facilitate self-evolution through optimization of the ambient environment, making it stable and habitable for life. The first and foremost goal of primordial metabolic networks was to obtain sufficient phosphorus. Sammox-driven sulfur biochemistry launched iron redox geochemistry; therefore, phosphite was liberated from ferruginous sediments[35], permitting biochemistry feedback to geochemistry. If and only if P reached a certain concentration in the Hadean oceans, sulfur biochemistry could lead to the emergence of phosphorus biochemistry, and the RNA world could have replaced the thioester world.

Our findings regarding Sammox-driven proto-anabolic networks suggested that primordial metabolic networks would rise from coupling transformation of C, H, O, N, S, and/or Fe at their earliest stage of the transition from geochemistry to biochemistry. The elements of the chemical components that supporting Sammox-driven

proto-anabolic networks ultimately became essential or trace elements of life, providing a strong explanation for the unique features of life. Exploration of Sammox provides a new perspective for understanding the emergence of biochemistry from geochemistry and highlights the fundamental significance of Sammox for the origins of life on planetary systems.

References

1. Falkowski, P. G., Fenchel, T. & Delong, E. F. The microbial engines that drive earth's biogeochemical cycles. *Science* **320**, 1034–1039 (2008).
2. Sousa, F. L. et al. Early bioenergetic evolution. *Philos. Trans. R. Soc. B-Biol. Sci.* **368**, (2013).
3. Weiss, M. C. et al. The physiology and habitat of the last universal common ancestor. *Nat. Microbiol.* **1**, (2016).
4. Moore, E. K. et al. Metal availability and the expanding network of microbial metabolisms in the Archaean eon. *Nat. Geosci.* **10**, 629–636 (2017).
5. Ljungdah, L., Irion, E. & Wood, H. G. Total synthesis of acetate from CO2. I. Co-methylcobyric acid and CO-(methyl)-5-Methoxybenzimidazolylcobamide as intermediates with *Clostridium thermoaceticum*. *Biochemistry* **4**, 2771–2780 (1965).
6. Kelley, D. S. et al. A serpentinite-hosted ecosystem: the lost city hydrothermal field. *Science* **307**, 1428–1434 (2005).
7. Lane, N. & Martin, W. F. The origin of membrane bioenergetics. *Cell* **151**,

1406–1416 (2012).

8. Wächtershäuser, G. Pyrite formation, the first energy source for life: a hypothesis. *Syst. Appl. Microbiol.* **10**, 207–210, (1988).

9. Wächtershäuser, G. Evolution of the first metabolic cycles. *PHAS J.* **1**, 200–204 (1990).

10. deDuve, C. Blueprint for a cell: the nature and origin of life. (Neil Patterson , 1991).

11. Evans, M. C. W., Buchanan, B. B. & Arnon, D. I. A new ferredoxin-dependent carbon reduction cycle in a photosynthetic bacterium. *Proc. Natl. Acad. Sci. U. S. A.* **55**, 928–934 (1966).

12. Smith, E. & Morowitz, H. J. Universality in intermediary metabolism. *Proc. Natl. Acad. Sci. U. S. A.* **101**, 13168–13173 (2004).

13. Muchowska, K. B. et al. Metals promote sequences of the reverse krebs cycle. *Nat. Ecol. Evol.* **1**, 1716–1721 (2017).

14. Varma, S. J. et al. Native iron reduces CO_2 to intermediates and end-products of the acetyl-CoA pathway. *Nat. Ecol. Evol.* **2**, 1019–1024 (2018).

15. Martin, W. & Russell, M. J. On the origin of biochemistry at an alkaline hydrothermal vent. *Philos. Trans. R. Soc. B-Biol. Sci.* **362**, 1887–1925 (2007).

16. Orgel, L. E. The implausibility of metabolic cycles on the prebiotic earth. *PLoS. Biol.* **6**, 5–13 (2008).

17. Braakman, R. & Smith, E. The emergence and early evolution of biological carbon-fixation. *PLoS Comput. Biol.* **8**, (2012).

18. Camprubi, E. et al. Iron catalysis at the origin of life. *IUBMB Life* **69**, 373–381 (2017).

19. Goldford, J. E. et al. Remnants of an ancient metabolism without phosphate. *Cell* **168**, 1126–1134 (2017).

20. Fdz-Polanco, F. et al. Combining the biological nitrogen and sulfur cycles in anaerobic conditions. *Water Sci. Technol.* **44**, 77–84 (2001).

21. Amend, J. P. et al. Energetics of chemolithoautotrophy in the hydrothermal system of Vulcano Island, southern Italy. *Geobiology* **1**, 37–58 (2003).

22. Philippot, P. et al. Early archaean microorganisms preferred elemental sulfur, not sulfate. *Science* **317**, 1534–1537 (2007).

23. Brandes, J. A. et al. Abiotic nitrogen reduction on the early earth. *Nature* **395**, 365–367 (1998).

24. Smirnov, A. et al. Abiotic ammonium formation in the presence of Ni-Fe metals and alloys and its implications for the hadean nitrogen cycle. *Geochem. Trans.* **9**, (2008).

25. Sleep, N. H. The hadean-archaean environment. *Cold Spring Harbor Perspect. Biol.* **2**, (2010).

26. Kuypers, M. et al. The microbial nitrogen-cycling network. *Nat. Rev. Microbiol.* **16**, 263–276 (2018).

27. Eigen, M. Self-organization of matter and the evolution of biological macromolecules. *Naturwissenschaften* **58**, 465–562 (1971).

28. Heinen, W. & Lauwers, A. M. Organic sulfur compounds resulting from the

interaction of iron sulfide, hydrogen sulfide and carbon dioxide in an anaerobic aqueous environment. *Orig. Life Evol. Biosph.* **26**, 131–150 (1996).

29. Yamaguchi, A. et al. Electrochemical CO_2 reduction by Ni-containing iron sulfides: how is CO_2 electrochemically reduced at bisulfide-bearing deep-sea hydrothermal precipitates? *Electrochim. Acta* **141**, 311–318 (2014).

30. Martin, W. F., Sousa, F. L. & Lane, N. Evolution energy at life's origin. *Science* **344**, 1092–1093 (2014).

31. Wächtershäuser, G. Before enzymes and templates-theory of surface metabolism. *Microbiol. Rev.* **52**, 452–484 (1988).

32. Shen, Y. A., Buick, R. & Canfield, D. E. Isotopic evidence for microbial sulphate reduction in the early Archaean era. *Nature* **410**, 77–81 (2001).

33. Mojzsis, S. J. et al.. Mass-independent isotope effects in Archean (2.5 to 3.8 Ga) sedimentary sulfides determined by ion microprobe analysis. *Geochim. Cosmochim. Acta* **67**, 1635–1658 (2003).

34. Eck, R. V. & Dayhoff, M. O. Evolution of the structure of ferredoxin based on living relics of primitive amino acid sequences. *Science* **152**, 363–366 (1966).

35. Herschy, B. et al. Archean phosphorus liberation induced by iron redox geochemistry. *Nat. Commun.* **9**, (2018).

36. Jorgensen, B. B. A thiosulfate shunt in the sulfur cycle of marine-sediments. *Science* **249**, (1990).

37. Clement, J. C. et al. Ammonium oxidation coupled to dissimilatory reduction of iron under anaerobic conditions in wetland soils. *Soil Biol. Biochem.* **37**,

2323–2328 (2005).

38. Yang, W. H., Weber, K. A. & Silver, W. L. Nitrogen loss from soil through anaerobic ammonium oxidation coupled to iron reduction. *Nat. Geosci.* **5**, 538–541 (2012).

39. Bao, P. & Li, G. X. Sulfur-driven iron reduction coupled to anaerobic ammonium oxidation. *Environ. Sci. Technol.* **51**, 6691–6698 (2017).

40. Postgate, J. R. The sulphate-reducing bacteria (Cambridge University, 1984).

41. Wacey, D. et al. Microfossils of sulphur-metabolizing cells in 3.4-billion-year-old rocks of Western Australia. *Nat. Geosci*. **4**, 698–702 (2011).

42. Crane, B. R. & Getzoff, E. D. The relationship between structure and function for the sulfite reductases. *Curr. Opin. Struct. Biol.* **6**, 744–756 (1996).

43. Bonomi, F., Werth, M. T. & Kurtz, D. M. Assembly of [FenSn(SR)]2-(n=2, 4) in aqueous media from iron salts, thiols and sulfur, sulfide, thiosulfide plus rhodonase. *Inorg. Chem.* **24**, 4331–4335 (1985).

44. Lefaou, A. et al. Thiosulfate, polythionates and elemental sulfur assimilation and reduction in the bacterial world. *FEMS Microbiol. Lett.* **75**, 351–382 (1990).

45. Bordo, D. & Bork, P. The rhodanese/Cdc25 phosphatase superfamily-sequence-structure-function relations. *EMBO Rep.* **3**, 741–746 (2002).

46. Zhuang, W. Q. et al. Incomplete wood-ljungdahl pathway facilitates one-carbon metabolism in organohalide-respiring *Dehalococcoides mccartyi.*

Proc. Natl. Acad. Sci. U. S. A. **111**, 6419–6424 (2014).

47. Mall, A. et al. Reversibility of citrate synthase allows autotrophic growth of a thermophilic bacterium. *Science* **359**, 563–567 (2018).

48. Huber, C. & Wächtershäuser, G. Activated acetic acid by carbon fixation on (Fe,Ni)S under primordial conditions. *Science* **276**, 245–247 (1997).

49. Lovelock, J. E. The Ages of Gaia (Oxford University, 1995).

Acknowledgements This research was financially supported by the National Natural Science Foundation of China (General Program Nos. 41571240 and 41571130063).

Competing interests The authors declare no competing interests.

Methods

Enrichment and isolation of Sammox bacterium.

Surface paddy soil mud (0–20 cm depth) in the upper section of a paddy field was collected from Guangxi Dahuanjiang region (24°53'52" N, 108°17'43" E), in the southwest of China. Soil materials were air-dried, ground with a mortar and crushed to pass through a 2.0 mm sieve for character determination. Soil organic carbon (19.81 g kg^{-1}) was determined by potassium dichromate oxidation titration, and soil total Fe (31.9 g kg^{-1}) was determined by ICP-OES. Plant available sulfur (29.1 mg kg^{-1}) was determined by turbidimetry. Ammonium was 120.5 mg kg^{-1}.

For enrichment, approximately 0.5 g of paddy soil was transferred to 100 ml of

double distilled water. After shaking, five milliliters of the suspension was inoculated into 100 ml of anaerobic freshwater medium[39,50] with additional sulfur (thiosulfate or sufate) (3.0 mM) and ammonium ($^{15}NH_4Cl$, 1.0 mM) and incubated statically for one week. The basal medium contained (g l^{-1}): KH_2PO_4 0.2, $MgCl{\cdot}6H_2O$ 0.4, $CaCl_2{\cdot}2H_2O$ 0.1, KCl 0.5. The trace elemental mixture contained (l^{-1}): double distilled water 987 ml, HCl (25%) 12.5 ml (100 mM), $FeCl_2{\cdot}4H_2O$ 957 mg (7.5 mM), H_3BO_3 30 mg (0.5 mM), $MnCl_2{\cdot}4H_2O$ 100 mg (0.5 mM), $CoCl_2{\cdot}6H_2O$ 190 mg (0.8 mM), $NiCl{\cdot}6H_2O$ 24 mg (0.1 mM), $CuCl_2{\cdot}2H_2O$ 2 mg (0.01 mM), $ZnSO_4{\cdot}7H_2O$ 144 mg (0.5 mM), $Na_2MoO_4{\cdot}2H_2O$ 36 mg (0.15 mM). Selenite-tungstate solution (l^{-1}): NaOH 0.4 g, $Na_2SeO_3{\cdot}5H_2O$ 6 mg, $Na_2WO_4{\cdot}2H_2O$ 8 mg. Bicarbonate solution $NaHCO_3$ 84 g l^{-1} 30 ml. The above mentioned stock solutions or aliquots were aseptically added to the basal medium (l^{-1}): trace element solution (1.0 ml), selenite-tungstate solution (0.1 ml), bicarbonate solution (10.0 ml), biotin, 4-aminobenzoic acid, 10 mg l^{-1} pantothenate, pyridoxamine, nicotinic acid and 20 mg l^{-1} thiamine, 5 ml l^{-1}; vitamin B_{12} solution with 50 mg l^{-1}, 1.0 ml l^{-1}. Sodium sulfate plus thiosulfate solution (1.0 ml, 3.0 mM final concentration) and ammonium (0.5 ml, 1.0 mM final concentration) were added into medium if necessary. The pH was adjusted to 8.0.

A volume of 0.5 ml of a positive Sammox culture, in which sulfur reduction coupled to anaerobic ammonium oxidation, was sub-inoculated onto Acidovorax complete agar medium under 5% CO_2 atmosphere. Single colony was selected and inoculated back into anaerobic freshwater medium. Positive Sammox samples were continuously sub-inoculated using the Acidovorax complete agar medium. A single

Sammox bacterium (designated GX3-BWBA) was isolated after sub-cultivation for five times, and was continuously cultivated for one year in anaerobic freshwater medium. The purity of GX3-BWBA was confirmed by promoting the growth of heterotrophic bacteria by addition of peptone and yeast extract to the defined freshwater mineral medium (data not shown)[51]. Finally, the purity of GX3-BWBA was confirmed by deep Illumina sequencing.

This study was performed using a series of experiments, for Sammox by GX3-BWBA: (I) 3.0 mM thiosulfate + 1.0 mM $^{15}NH_4Cl$, (II) 3.0 mM thiosulfate + 1.0 mM $^{15}NH_4Cl$ + GX3-BWBA, (III) 3.0 mM sulfate + 1.0 mM $^{15}NH_4Cl$, (IV) 3.0 mM sulfate + 1.0 mM $^{15}NH_4Cl$ + GX3-BWBA. Experiments started and were sampled at the sampled at the 0, 3, 6, 9, 12, 15, 18, 21, 24, 27, 34 day. Experiments were performed anaerobically in 100-ml serum bottles in the dark at 30 ^{o}C. Each batch of experiments was established in triplicate, inoculated with 1.0 ml GX3-BWBA exponential phase culture if necessary.

Genome sequencing and assembly

The genome of *R. thioammoniphilus* (strain GX3-BWBA) was sequenced using an Illumina HiSeq 4000 system (Illumina, SanDiego, CA, USA) at the Beijing Genomics Institute (Shenzhen, China). Genomic DNA was sheared randomly to construct three read libraries with lengths of (150:150) by a Bioruptor ultrasonicator (Diagenode, Denville, NJ, USA) and physico-chemical methods. The paired-end fragments libraries were sequenced according to the Illumina HiSeq 4000 system's protocol. Raw reads of low quality from paired-end sequencing (those with

consecutive bases covered by fewer than five reads) were discarded. The sequenced reads were assembled using SOAPdenovo v1.05 software. This Whole Genome Shotgun project has been deposited at DDBJ/ENA/GenBank under the accession QMKS00000000. The version described in this paper is version QMKS01000000.

Genome Component prediction

Gene prediction was performed on the *R. thioammoniphilus* genome assembly by glimmer3 (http://www.cbcb.umd.edu/software/glimmer/) with Hidden Markov models. tRNA, rRNA and sRNAs recognition made use of tRNAscan-SE[52], RNAmmer, and the Rfam database. The tandem repeats annotation was obtained using the Tandem Repeat Finder (http://tandem.bu.edu/trf/trf.html), and the minisatellite DNA and microsatellite DNA selected based on the number and length of repeat units. The Genomic Island Suite of Tools (GIST) used for genomic islands analysis (http://www5.esu.edu/cpsc/bioinfo/software/GIST/) with Island Path-DIOMB, SIGI-HMM, Island Picker method. Prophage regions were predicted using the PHAge Search Tool (PHAST) web server (http://phast.wishartlab.com/) and CRISPR identification using CRISPRFinder.

Protein sequences will be downloaded from NCBI, and get sequences in the taxonomy of species classification information; The sequences using mafft software for multiple sequence alignment. After comparing the sequences, using Fasttree software construct phylogenetic tree (neighbor joining algorithm). Using R language ggtree package for visualization mapping.

Gene annotation and protein classification

The best hit abstracted using Blast alignment tool for function annotation. Seven databases which are KEGG (Kyoto Encyclopedia of Genes and Genomes), COG (Clusters of Orthologous Groups), NR (Non-Redundant Protein Database databases), Swiss-Prot[53], and GO (Gene Ontology), TrEMBL, EggNOG are used for general function annotation. Representative metabolic gene clusters were displayed with Easyfig[54].

General procedure for prebiotic Sammox-driven CO_2 fixation

Each 50 ml basal solution was transferred into 60 ml serum bottles and sealed with butyl rubber stoppers and aluminium crimp caps. The solution was autoclaved and cooled as room temperature after washed by He gas (purity=99.999%). Additional trace elemental mixture solutions were filter sterilized or autoclaved individually. Additional sulfur (thiosulfate or sufate) (3.0 mM) and/or ammonium (NH_4Cl, 1.0 mM) was added into serum bottle. The mixed solution was termed as Sammox reaction system.

The above mentioned stock solutions or aliquots were aseptically added to the basal medium (l^{-1}): trace element solution (2.0 ml), selenite-tungstate solution (0.2 ml), bicarbonate solution (10.0 ml). Sodium sulfate, thiosulfate (1.0 ml), ammonium solution (0.5 ml), and fresh precipitated Fe-S mineral were added into medium if necessary. Serum bottles were kept 100 ^{o}C in a water bath in the dark for 24 h, then maintain at 70 ^{o}C in the dark for another 24 h, and sampling at 48 h to determinate organic products.

This study was performed using a series of experiments: (I) 3.0 mM thiosulfate +

1.0 mM NH_4Cl + 20 mM HCO_3^-, (II) 3.0 mM thiosulfate + 1.0 mM NH_4Cl + 20 mM HCO_3^- + 1.0 mM Fe-S, (III) 3.0 mM thiosulfate + 20 mM HCO_3^-, (IV) 3.0 mM sulfate + 1.0 mM NH_4Cl + 20 mM HCO_3^-, (IV) 3.0 mM sulfate + 1.0 mM NH_4Cl + 20 mM HCO_3^- + 1.0 mM Fe-S, (V) 3.0 mM sulfate + 20 mM HCO_3^-, (VI) 1.0 mM NH_4Cl + 20 mM HCO_3^-.

General procedure for thiol/thioester promoted Sammox-driven CO_2 fixation.

A solution of methanethiol was added to Sammox reaction system. The reaction systems were heated at 100 ^oC in a water bath in the dark for 24 h, then maintain at 70 ^oC in the dark for another 24 h, and removed from the water bath and allowed to cool to room temperature before derivatization and gas chromatography–mass spectrometry analysis.

This study was performed using a series of experiments: (I) 3.0 mM thiosulfate + 1.0 mM NH_4Cl + 20 mM HCO_3^- + 0.8 mM methanethiol, (II) 3.0 mM thiosulfate + 1.0 mM NH_4Cl + 20 mM HCO_3^- + 1.0 mM Fe-S + 0.8 mM methanethiol, (III) 3.0 mM sulfate + 1.0 mM NH_4Cl + 20 mM HCO_3^- + 0.8 mM methanethiol, (IV) 3.0 mM sulfate + 1.0 mM NH_4Cl + 20 mM HCO_3^- + 1.0 mM Fe-S + 0.8 mM methanethiol.

General procedure for verification of Sammox-driven combination of reductive acetyl-CoA pathway and incomplete rTCA cycle.

We design this experimental set to verify if Sammox-driven reductive acetyl-CoA pathway could go into Sammox-driven incomplete rTCA cycle. The general procedure is the same as above. Pyruvate (1.0 mM, final concentration) was added into Sammox reaction system as substrate. Serum bottles were heated at 100 ^oC

in a water bath in the dark for 24 h, then maintain at 70 ^{o}C in the dark for another 24 h, and allowed to cool to room temperature before derivatization and gas chromatography–mass spectrometry analysis.

This study was performed using a series of experiments: (I) 3.0 mM thiosulfate + 1.0 mM NH_4Cl + 20 mM HCO_3^- + 1.0 mM pyruvate + 1.0 mM Fe-S + methanethiol, (II) 3.0 mM thiosulfate + 1.0 mM NH_4Cl + 20 mM HCO_3^- + 1.0 mM Fe-S + 1.0 mM pyruvate, (III) 3.0 mM thiosulfate + 1.0 mM NH_4Cl + 20 mM HCO_3^- + 1.0 mM pyruvate, (IV) 3.0 mM thiosulfate + 20 mM HCO_3^- + 1.0 mM pyruvate, (V) 3.0 mM sulfate + 1.0 mM NH_4Cl + 20 mM HCO_3^- + 1.0 mM Fe-S + 1.0 mM pyruvate + methanethiol, (VI) 3.0 mM sulfate + 1.0 mM NH_4Cl + 20 mM HCO_3^- + 1.0 mM Fe-S + 1.0 mM pyruvate, (VII)3.0 mM sulfate + 1.0 mM NH_4Cl + 20 mM HCO_3^- + 1.0 mM pyruvate, (VIII) 3.0 mM sulfate + 20 mM HCO_3^- + 1.0 mM pyruvate, (IX) 1.0 mM NH_4Cl + 20 mM HCO_3^- + 1.0 mM pyruvate.

Chemicals

All reagents and solvents were purchased from commercial suppliers and used without further purification unless otherwise noted.

Sampling analytical methods

(i) **Enumeration of microbe viable counts.** The spread-agar-plate method was used for enumeration of bacterial counts in GX3-BWBA culture[55]. The Acidovorax complete agar medium, pH 7.0, contained 5.0 g l^{-1} peptone (Difco), 3.0 g l^{-1} beef extract and 15 g l^{-1} agar (Difco). A 50 µl sample was taken from GX3-BWBA culture at the 0, 3, 6, 9, 12, 15, 18, 21, 24, 27 and 34 days and inoculated onto plates for cell

counting. Visible colonies produced on the agar plate were counted at 48 h. Bacterial numbers were expressed as colony-forming units (CFU) per milliliter of culture[55].

(ii) **Electron microscopy.** Morphology of GX3-BWBA was investigated by transmission electron microscope (TEM) (TEM, HITACHI H-7500). Cells from the culture were collected by centrifugation, washed and diluted with phosphate buffer (pH 7.5), and dropped on to specimens. The material was examined after dry by airing.

(iii) **Sulfide.** The analysis of sulfide in filtered samples was performed photometrically by the methylene blue method[56]. Absorption at 660 nm was measured (Infinite 200PRO; TECAN).

(iV) **Sulfate, sulfite, nitrite, acetate, formate and ammonium.** To determine sulfate, sulfite, nitrite, acetate and formate, 0.5 ml of the sample was filtered (0.22 μm) to remove particulates that could interfere with ion chromatography. The ion chromatography system consisted of an ICS-5000^{+} SP pump (Thermo Fisher Scientific Inc. Sunnyvale, CA, USA), a column oven ICS-5000^{+} DC, an electrochemical detector DC-5. The ion chromatography column system used a Dionex Ionpac AS11-HC column. The operating condition was with an eluent of 30 mM KOH at a flow rate of 1.0 ml min^{-1}. For determination of ammonium, the ion chromatography column system used a Dionex Ionpac CS12A column.

(V) **Thiosulfate.** Thiosulfate was determined by an Agilent 1260 infinity HPLC system, equipped with a quaternary pump (Agilent, USA). Thiosulfate was separated by a Zorbax SB-C18 column (150×4.6 mm, 5 μm), and detected by using of

DAD detector at 215 nm. All analyses were performed at 40 °C with a flow rate of 1 ml min^{-1}. Na_2HPO_4 was used as solvent. The pH of the solvent was adjusted with 1.0 M HCl. Samples were filtered through 0.45 μm Cosmonice Filters (Millipore, Tokyo, Japan) and immediately injected into the HPLC system[57].

(Vi) Gas Analysis. At each sampling time point, each serum bottle was shaken vigorously to equilibrate the N_2 between dissolved and gas phases. Dinitrogen sampling and determination was performed according to a literature procedure[39].

(Vii) Derivatization procedure and product identification

For optimal GC resolution, the carboxylic acids were converted to ethyl esters using a mixture of ethanol/ethyl chloroformate (EtOH/ECF). Derivatization of carboxylic acids to esters was performed according to a literature procedure[13]. Reaction products derivatized to ethyl esters of carboxylic acids were identified by comparing the mass spectra and retention times against analogously derivatized authentic samples. ECF derivatization was preferred for small molecule substrates (pyruvate, lactate, malate, fumarate, succinate, α-ketoglutarate, amino acid). The carboxylic acids might also convert to methyl esters using a mixture of methanol/methyl chloroformate (MeOH/MCF), following the same procedure to ECF derivatization to detect *cis*-aconitate, tricarballylate, isocitrate and citrate.

(Viii) Gas chromatography–mass spectrometry (GC–MS**) analysis for rTCA metabolites determination.**

GC–MS analysis was performed on a GC System 7890B connected to a MSD block 5977A, using Agilent High Resolution Gas Chromatography Column: PN

19091S–433, HP–5MS, 28 m×0.25 mm, 0.25 Micron, SN USN 462366H. Samples were prepared in ethyl acetate (200 μl sample volume). The analysis was carried out on a splitless 1 μl injection volume with an injection port temperature 250 °C. Column oven temperature program was as follows: 60 °C for 1.0 min, ramped at 30 °C min^{-1} to 310 °C with 3.0 min hold, with a total running time of 12.33 min. The mass spectrometer was turned on after 3 min and was operated at the electron ionization mode with quadrupole temperature of 150 °C. Data acquisition was performed in the full-scan mode (50-500). Hydrogen (99.999 % purity) was used as carrier gas at a constant flow rate of 1.5 ml min^{-1}.

50. Strous, M. et al. Deciphering the evolution and metabolism of an anammox bacterium from a community genome. *Nature* **440**, 790–794 (2006).

51. Konneke, M. et al. Isolation of an autotrophic ammonia oxidizing marine archaeon. *Nature* **437**, 543–546 (2005).

52. Lowe, T. M. & Eddy, S. R. tRNAscan-SE: a program for improved detection of transfer RNA genes in genomic sequence. *Nucl. Acids Res*. **25** (5), 0955–0964 (1997).

53. Torto-Alalibo, T., Collmer, C. W. & Gwinn-Giglio, M. The plant-associated microbe gene ontology (PAMGO) consortium: community development of new gene ontology terms describing biological processes involved in microbe-host interactions. *BMC microbiol.* **9** (suppl 1), (2009).

54. Sullivan, M. J., Nicola K. P. & Scott A. B. Easyfig: a genome comparison

visualizer. *Bioinformatics* **27** (7), 1009–1010 (2011).

55. Kataoka, N. et al. Enrichment culture and isolation of slow growing bacteria. Appl. Microbiol. *Biotechnol*. **45**, 771–777 (1996).

56. Cline, J. D. Spectrophotometric determination of hydrogen sulfide in natural waters. imnol. *Oceanogr*. **14** (3), 454−458 (1969).

57. Kondo, R. et al. Determination of thiosulfate in a meromictic lake. *Fisheries Sci*. **66**, 1076–1081 (2000).

Legends of figures

Figure. 1 Sammox-driven proto-anabolic networks under hydrothermal conditions. Treatments were as follows (**a**, thiosulfate; **b**, sulfate): (i) sulfurous species, ammonium, Fe-S minerals, and thiols; (ii) sulfurous species, ammonium, and Fe-S minerals; (iii) sulfurous species, ammonium, and thiols; (iv) sulfurous species and ammonium; (v) ammonium; (vi) sulfurous species (see experimental details). The bar chart shows the yield of formate, acetate, succinate and α-ketoglutarate in each treatment group after 48 h. Error bars represent standard deviations of three replicates.

Figure. 2 Sammox-driven incomplete rTCA with pyruvate amendment under hydrothermal conditions. Treatments were as follows (**a**, thiosulfate; **b**, sulfate): (i) sulfurous species, ammonium, Fe-S minerals, and thiols; (ii) sulfurous species, ammonium, and Fe-S minerals; (iii) sulfurous species, ammonium, and thiols; (iv) sulfurous species and ammonium; (v) ammonium; (vi) sulfurous species (see experimental details). The bar chart shows the concentration of pyruvate, succinate and α-ketoglutarate in each treatment group after 48 h. Error bars represent standard deviations of three replicates.

Figure. 3 Hypothetical prebiotic reductive acetyl-CoA pathway powered by Sammox, **a**. Hypothetical proto-anabolic networks, a combination of acetyl-CoA pathway together with incomplete rTCA cycle powered by Sammox, and the role of its intermediates as universal biosynthetic precursors. Bar represents the final step of incomplete rTCA cycle, **b**. Conceptual model of Sammox-driven the origin of not

free-living organic precursor on the surface of iron-sulfur minerals in Hadean alkaline hydrothermal systems. Cubes represent iron-sulfur minerals/metals alloy. Globes represent the not free-living organic precursor, ligand sphere, **c**.

Figure. 4 Characters of *R. thioammoniphilus* strain GX3-BWBA. **a**, TEM image of cells. Scale bar represents 0.2 μm. **b**, Growth of GX3-BWBA under combined condition of ammonium and sulfurous species, with bicarbonate as sole carbon sources. Phylogenetic tree constructed by the maximum likelihood method, using 1478 nucleotides from 16S rDNA sequences, showing the position of strain GX3-BWBA in relation to members of the genus Ralstonia. The bar represents 0.1 changes per nucleotide position, **c**. Production rate of isotopically labeled dinitrogen for thiosulfate and sulfate-fueled Sammox by *R. thioammoniphilus* strain GX3-BWBA (**d**, **e**).

Figure. 5 Thiosulfate- and sulfate-fueled Sammox by *R. thioammoniphilus* strain GX3-BWBA. **a**, thiosulfate and reduction products. **b**, ammonium oxidation and products in thiosulfate-fueled Sammox. **c,** sulfate and reduction products (sulfide and sulfite as products of sulfate in control group are below detection limit). **d**, ammonium oxidation and products in sulfate-fueled Sammox. Error bars represent standard deviations of three biological replicates.

Figure. 6 Representative metabolic gene clusters from *R. thioammoniphilus* strain GX3-BWBA (**a**). The standard configuration of metabolic gene clusters (MGCs) in primary metabolism located in two scaffolds. MGCs contain enzymes of CO_2 fixation genes, including 31 rTCA cycle, and 30 reductive acetyl-CoA pathway genes,

6 dissimilatory sulfur metabolic genes, and 5 nitrification genes. Gene size and spacing are not to scale. Each gene was not condensed lie in genome. Protein phylogenetic tree derived from 26443 amino acid sequences of sulfite/nitrite reductase (**b**). Scale bars represent estimated sequence divergence or amino acid changes. Archaea, Bacteria, Eukaryota.

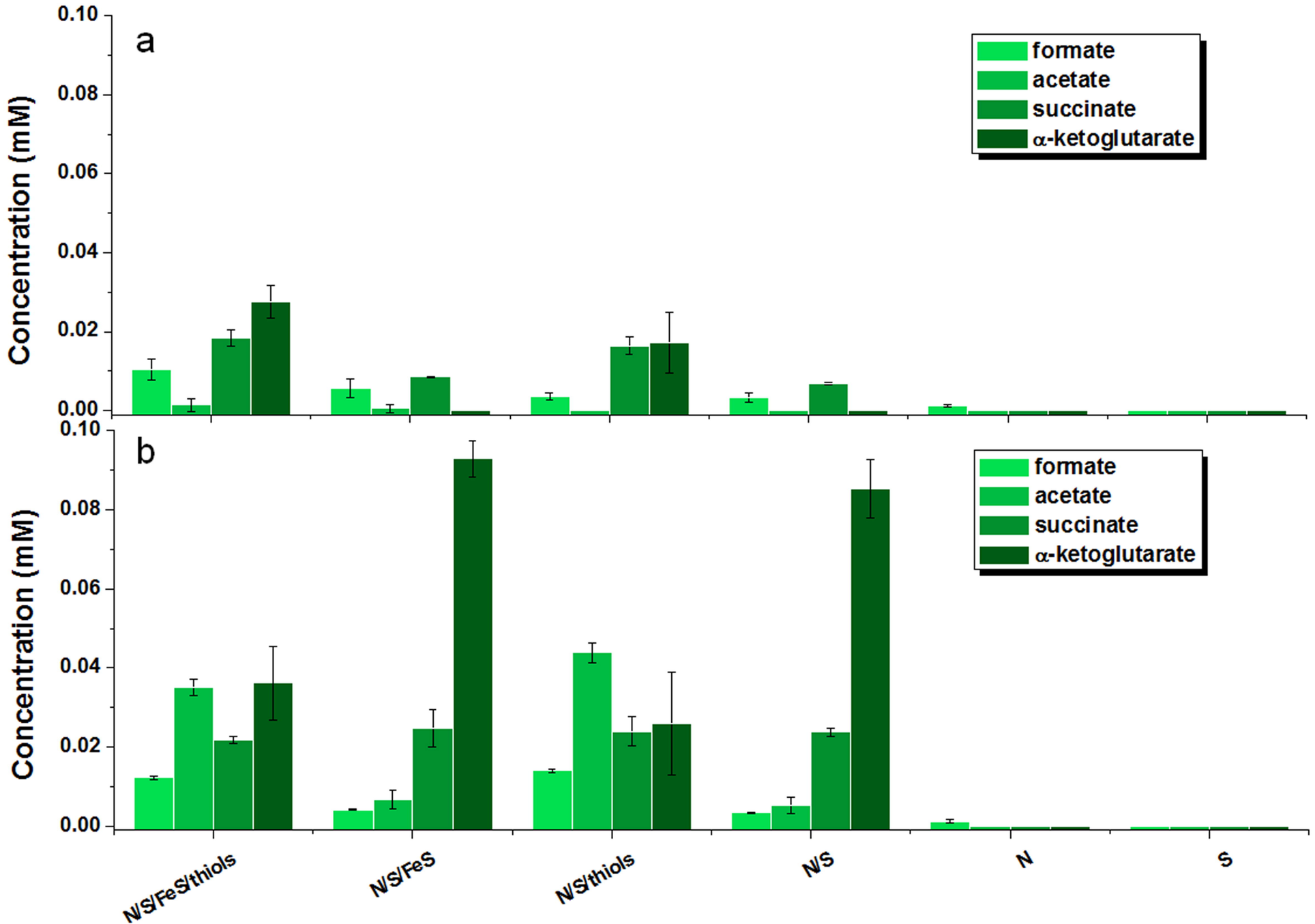
a
b
Concentration (mM)
0.00
0.02
0.04
0.06
0.08
0.10
formate
acetate
succinate
α-ketoglutarate
N/S/FeS/thiols
N/S/FeS
N/S/thiols
N/S
N
S

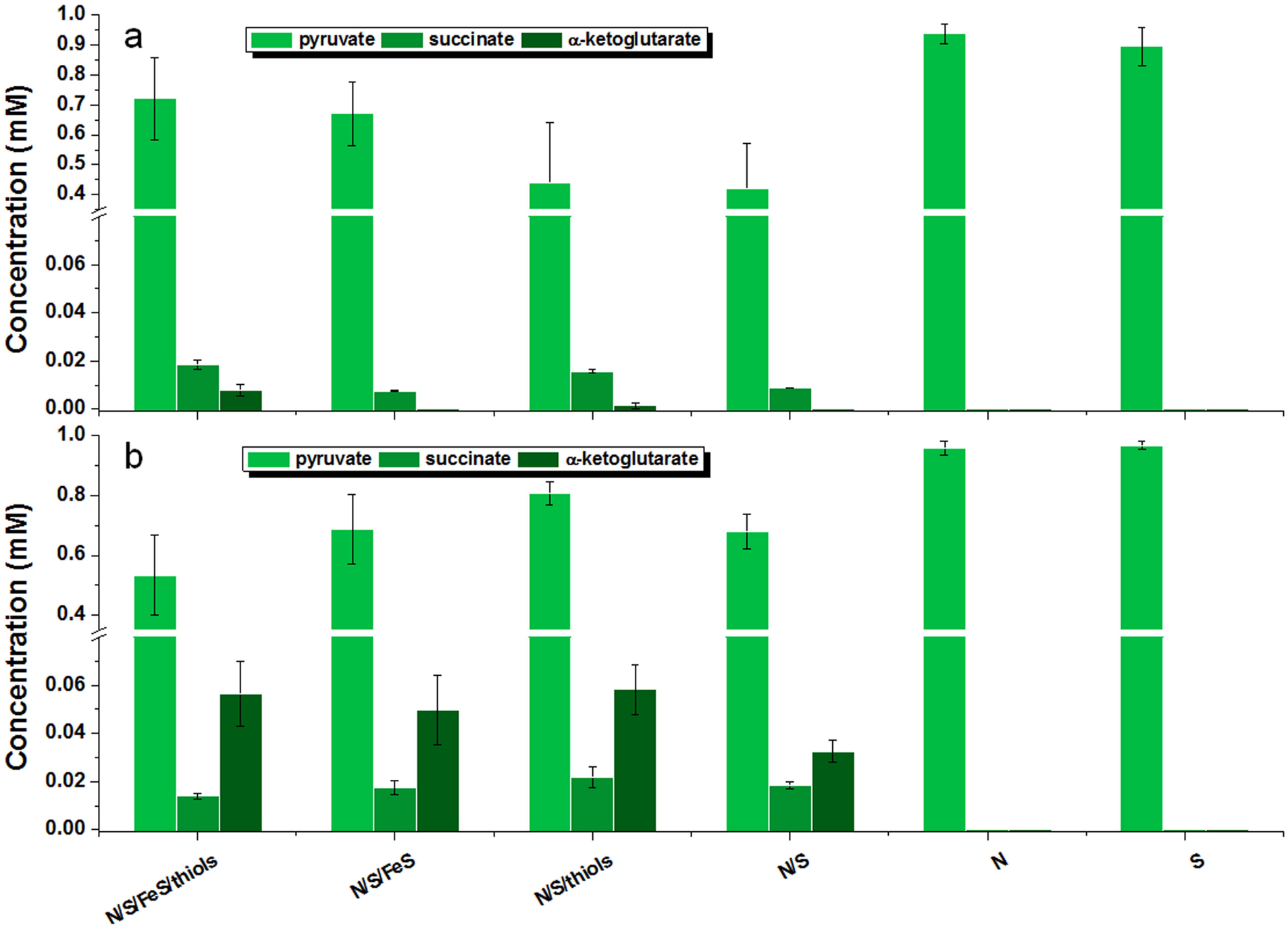
a
pyruvate
succinate
α-ketoglutarate
Concentration (mM)
1.0
0.9
0.8
0.7
0.6
0.5
0.4
0.06
0.04
0.02
0.00
b
pyruvate
succinate
α-ketoglutarate
Concentration (mM)
1.0
0.8
0.6
0.4
0.06
0.04
0.02
0.00
N/S/FeS/thiols
N/S/FeS
N/S/thiols
N/S
N
S

a

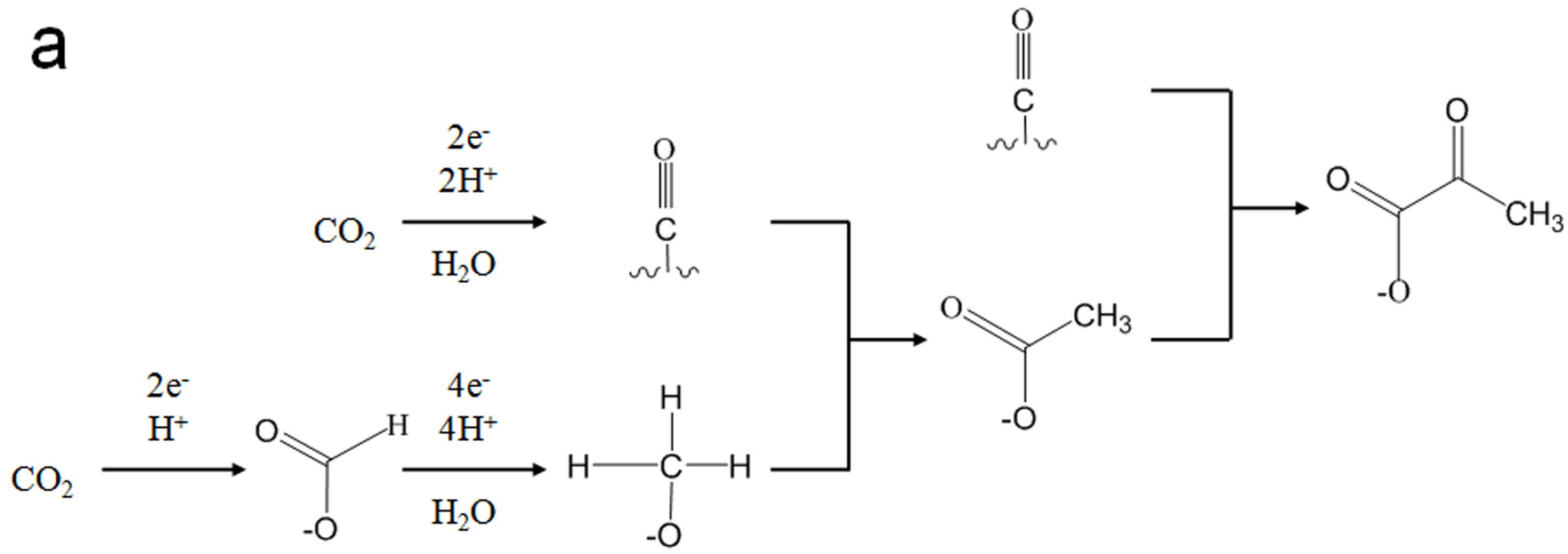
CO2
2e-
H+
4e-
4H+
H2O
2e-
2H+
H2O
CH3

b

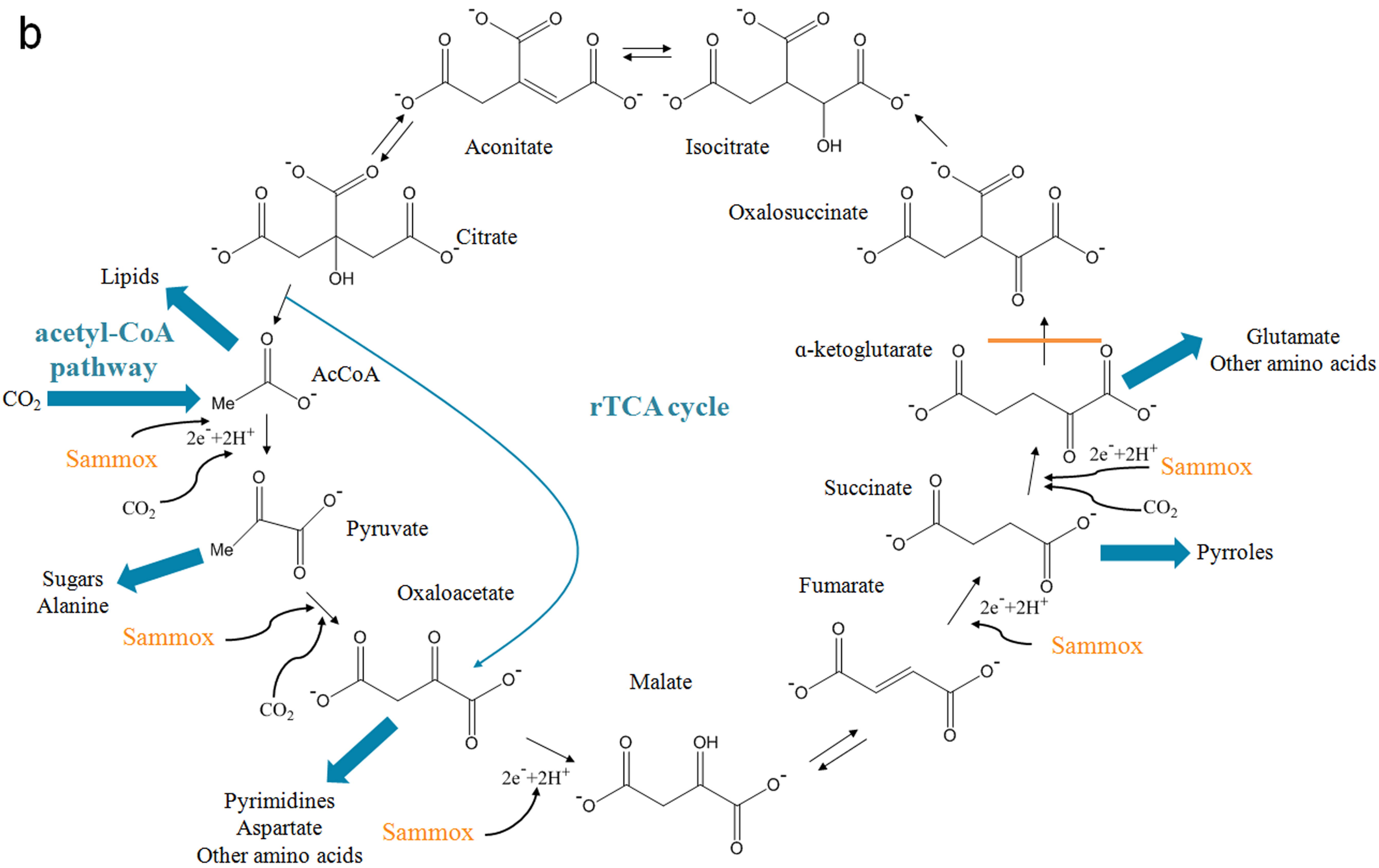
Aconitate
Isocitrate
Citrate
Oxalosuccinate
Lipids
acetyl-CoA pathway
CO2
AcCoA
Sammox
2e-+2H+
CO2
Pyruvate
Sugars
Alanine
Oxaloacetate
Sammox
CO2
rTCA cycle
α-ketoglutarate
Glutamate
Other amino acids
2e-+2H+
Sammox
Succinate
CO2
Pyrroles
Fumarate
2e-+2H+
Sammox
Malate
2e-+2H+
Sammox
Pyrimidines
Aspartate
Other amino acids

c

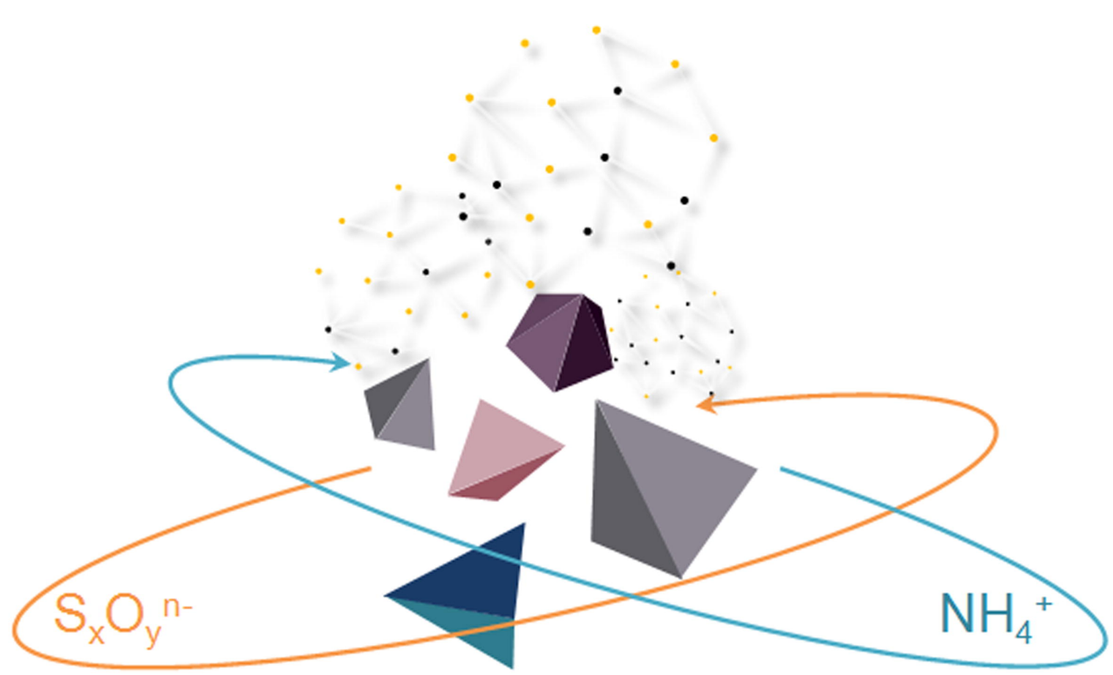
SxOyn-
NH4+

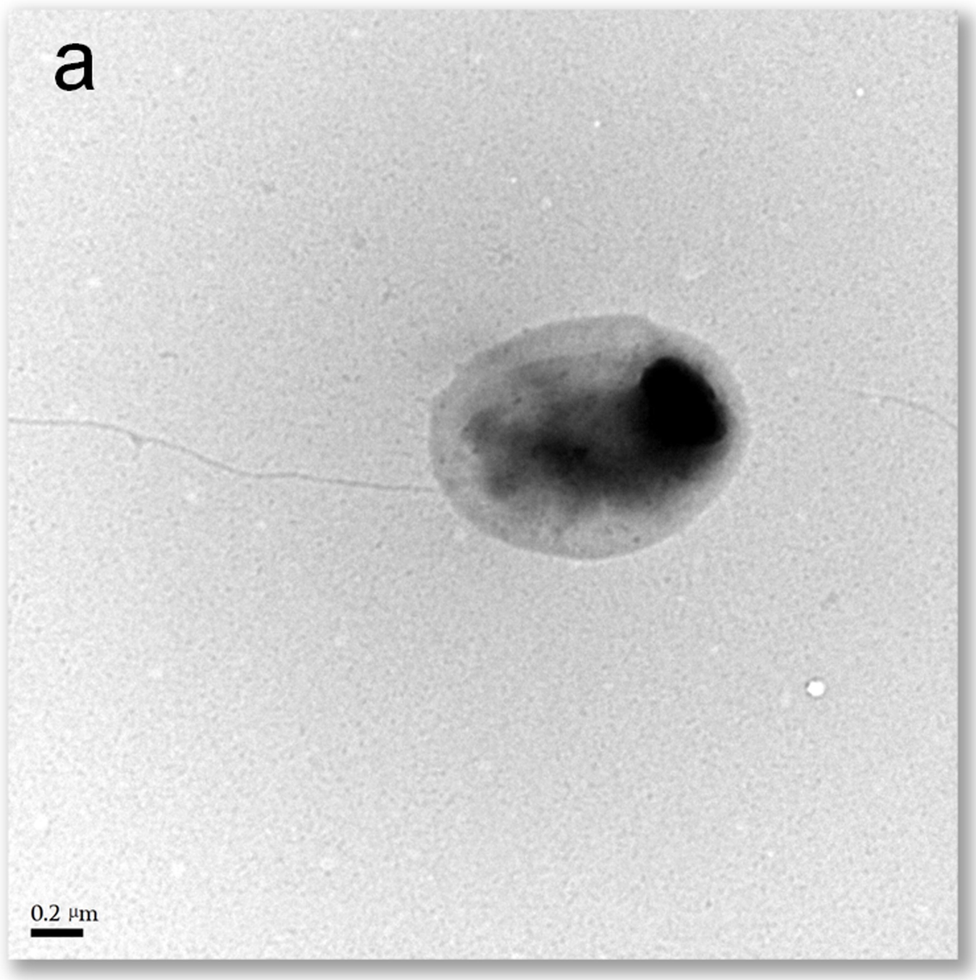
a
0.2 μm

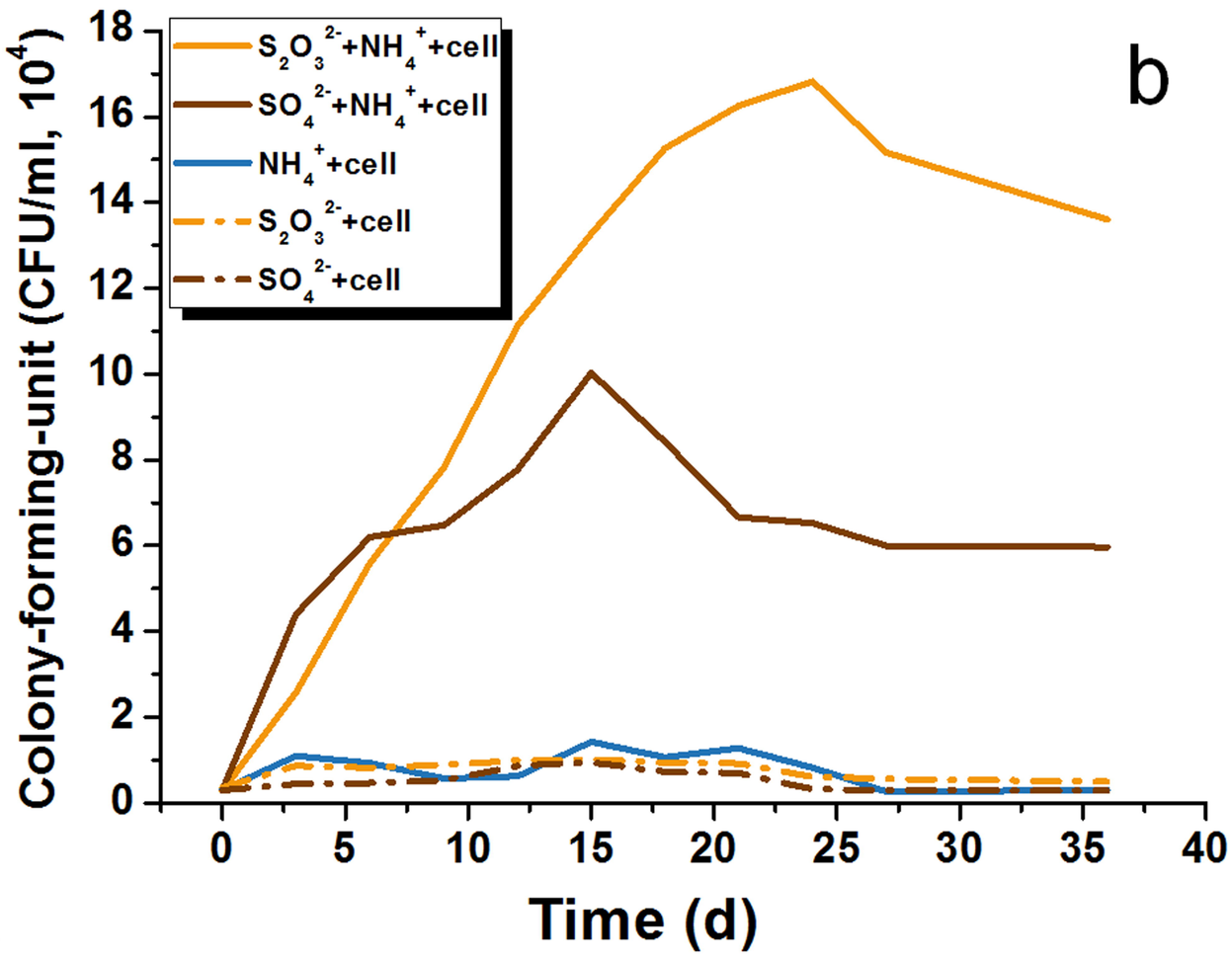
b
Colony-forming-unit (CFU/ml, 10^4)
Time (d)
S2O3 2-+NH4 +cell
SO4 2-+NH4 +cell
NH4 +cell
S2O3 2-+cell
SO4 2-+cell
0
2
4
6
8
10
12
14
16
18
0
5
10
15
20
25
30
35
40

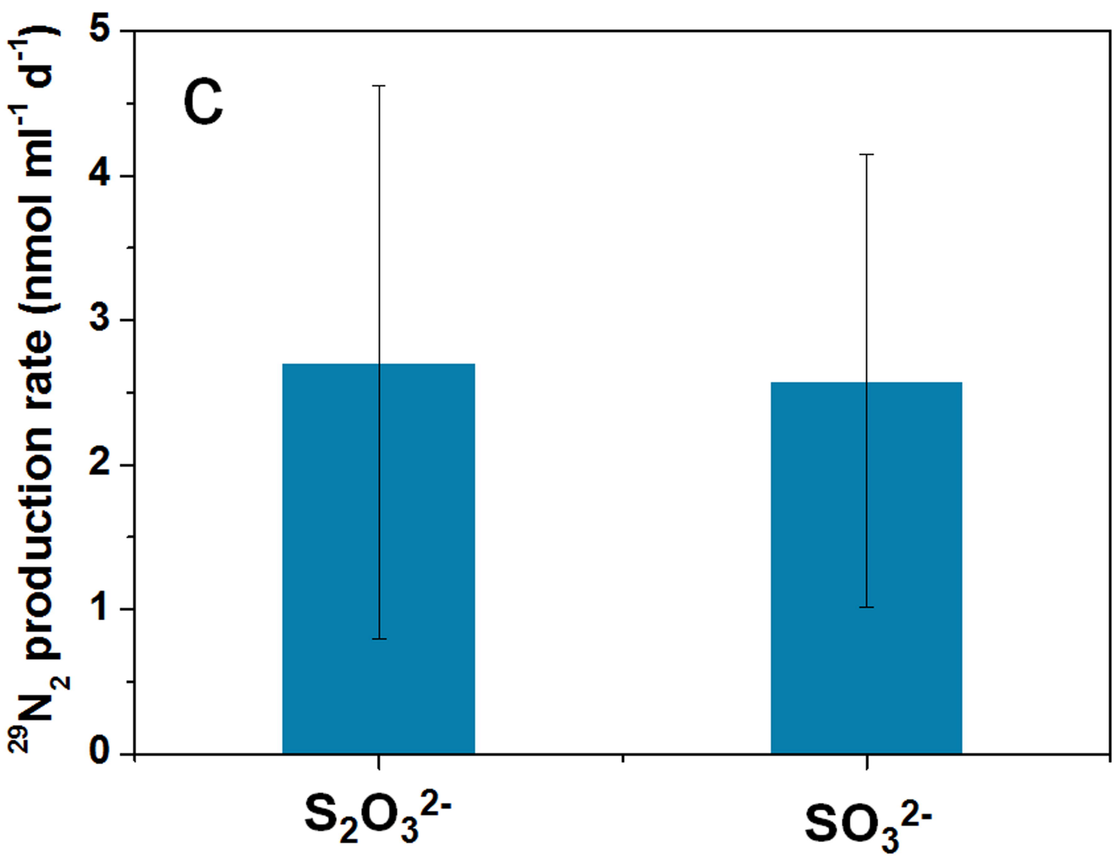
c
29N2 production rate (nmol ml-1 d-1)
S2O3 2-
SO3 2-
0
1
2
3
4
5

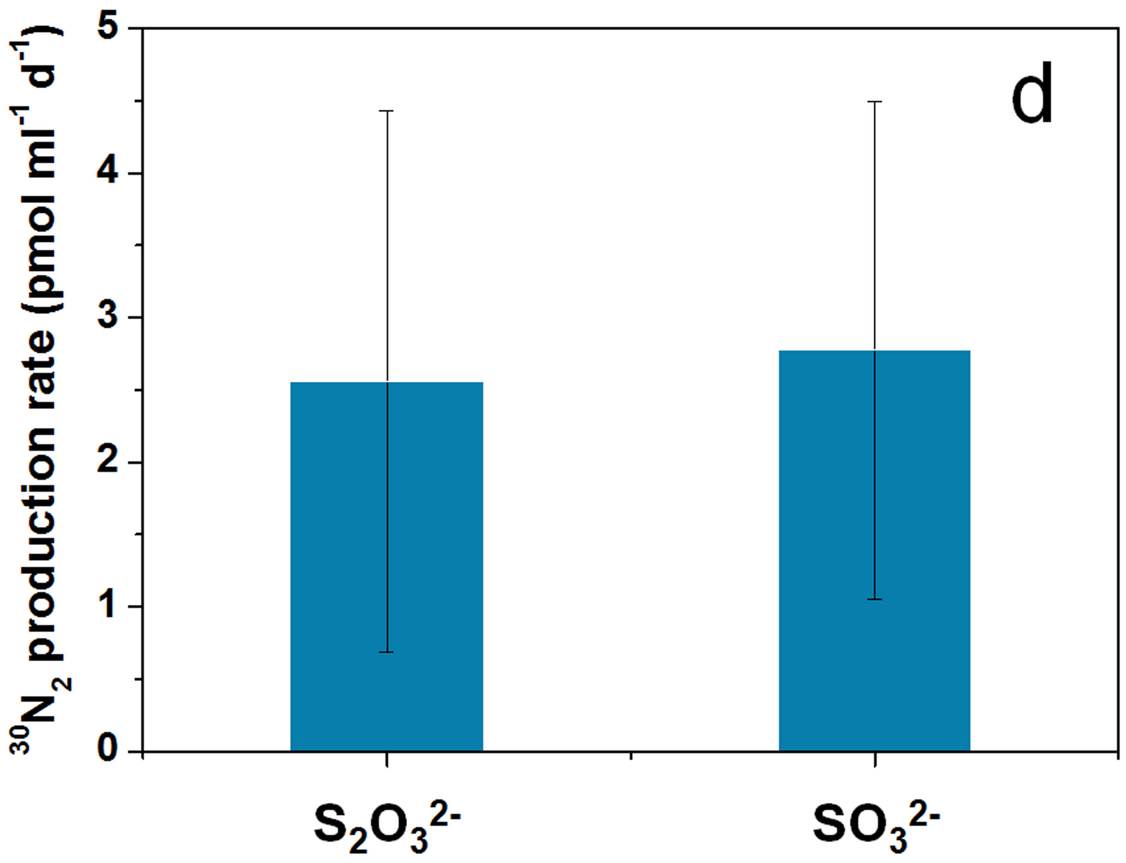
d
30N2 production rate (pmol ml-1 d-1)
S2O3 2-
SO3 2-
0
1
2
3
4
5

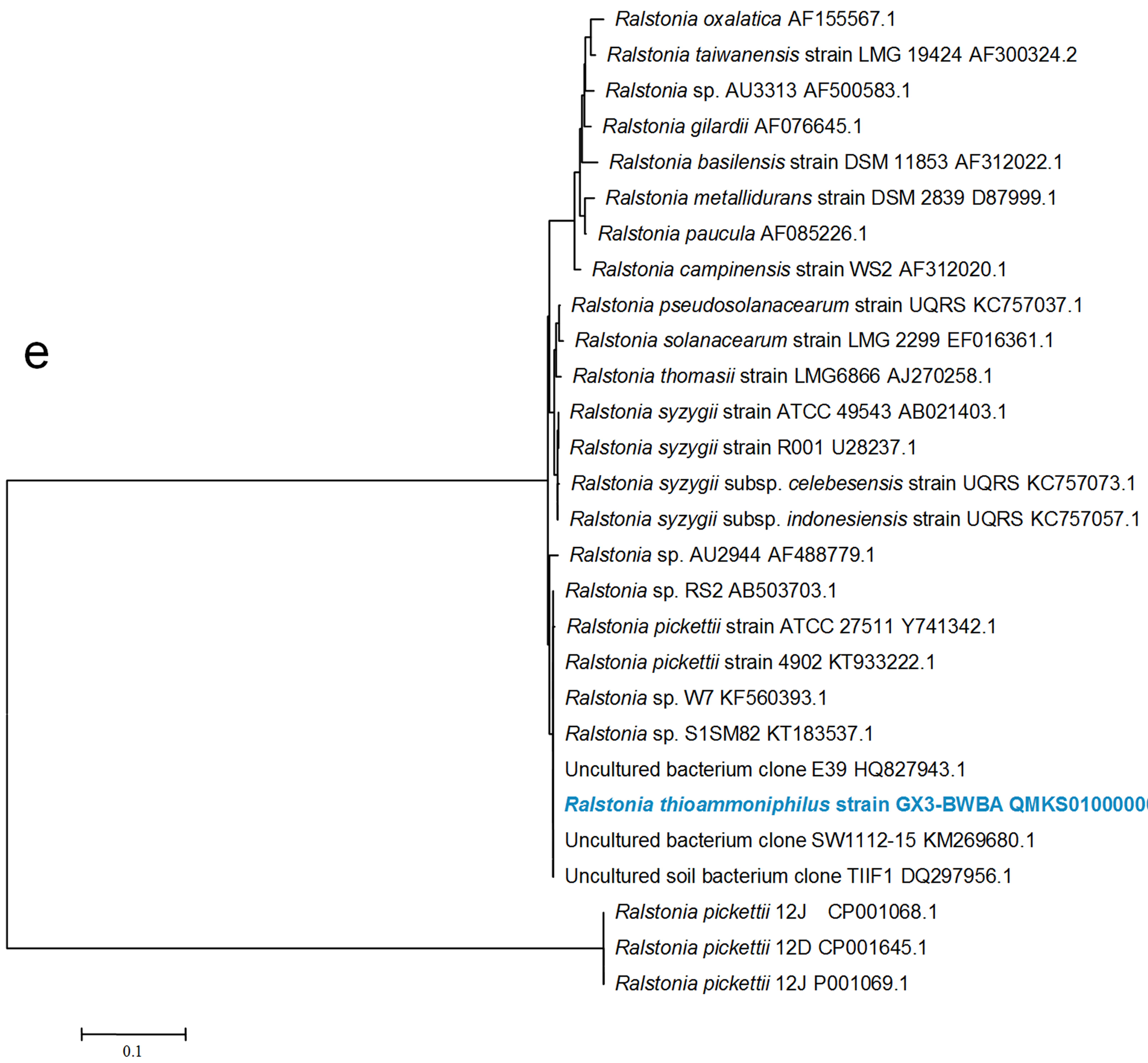
e
Ralstonia oxalatica AF155567.1
Ralstonia taiwanensis strain LMG 19424 AF300324.2
Ralstonia sp. AU3313 AF500583.1
Ralstonia gilardii AF076645.1
Ralstonia basilensis strain DSM 11853 AF312022.1
Ralstonia metallidurans strain DSM 2839 D87999.1
Ralstonia paucula AF085226.1
Ralstonia campinensis strain WS2 AF312020.1
Ralstonia pseudosolanacearum strain UQRS KC757037.1
Ralstonia solanacearum strain LMG 2299 EF016361.1
Ralstonia thomasii strain LMG6866 AJ270258.1
Ralstonia syzygii strain ATCC 49543 AB021403.1
Ralstonia syzygii strain R001 U28237.1
Ralstonia syzygii subsp. celebesensis strain UQRS KC757073.1
Ralstonia syzygii subsp. indonesiensis strain UQRS KC757057.1
Ralstonia sp. AU2944 AF488779.1
Ralstonia sp. RS2 AB503703.1
Ralstonia pickettii strain ATCC 27511 Y741342.1
Ralstonia pickettii strain 4902 KT933222.1
Ralstonia sp. W7 KF560393.1
Ralstonia sp. S1SM82 KT183537.1
Uncultured bacterium clone E39 HQ827943.1
Ralstonia thioammoniphilus strain GX3-BWBA QMKS01000000
Uncultured bacterium clone SW1112-15 KM269680.1
Uncultured soil bacterium clone TIIF1 DQ297956.1
Ralstonia pickettii 12J CP001068.1
Ralstonia pickettii 12D CP001645.1
Ralstonia pickettii 12J P001069.1
0.1

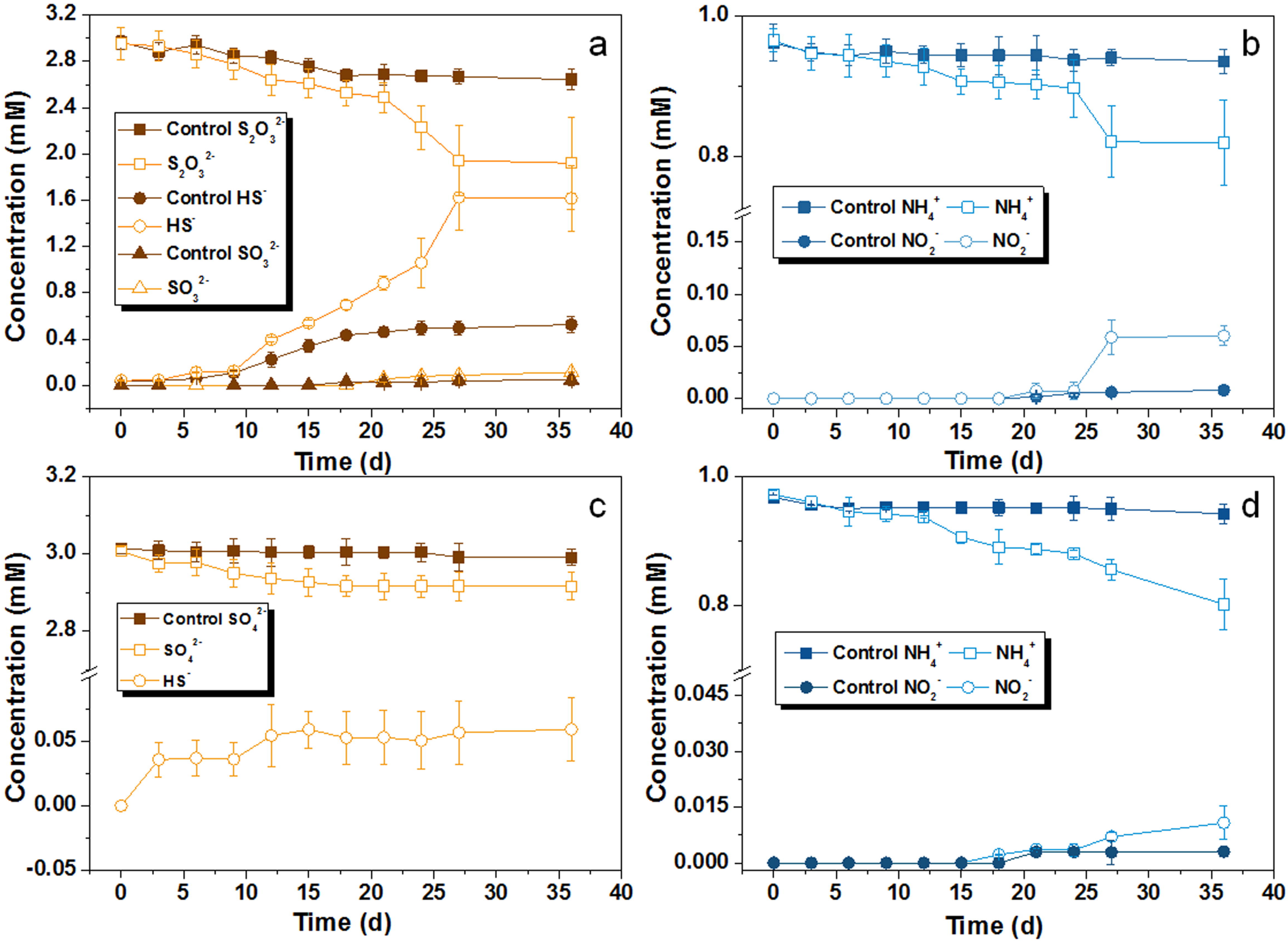
a
Concentration (mM)
Time (d)
Control $S_2O_3^{2-}$
$S_2O_3^{2-}$
Control HS^-
HS^-
Control SO_3^{2-}
SO_3^{2-}
b
Control NH_4^+
NH_4^+
Control NO_2^-
NO_2^-
c
Control SO_4^{2-}
SO_4^{2-}
HS^-
d

a

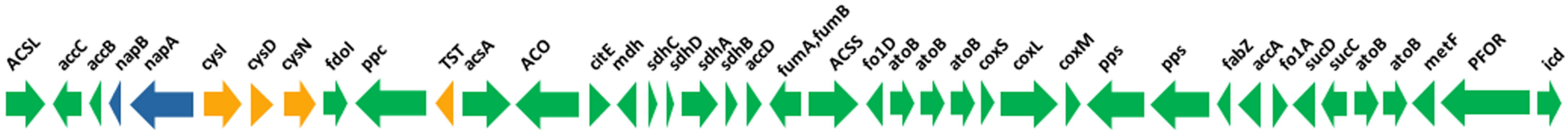
ACSL
accC
accB
napB
napA
cysI
cysD
cysN
fdoI
ppc
TST
acsA
ACO
citE
mdh
sdhC
sdhD
sdhA
sdhB
accD
fumA,fumB
ACSS
fo1D
atoB
atoB
atoB
coxS
coxL
coxM
pps
pps
fabZ
accA
fo1A
sucD
sucC
atoB
atoB
metF
PFOR
icd

fumC
sdhB
sdhB
sdhA
sdhD
sdhC
acnB
ACSS
pps
sdhB
k00666
pps
ackA
pta
cysJ
K00666
ACSS
fumC
aprB
nosZ
nirK
norB
ACSL
ACSS
pps
mdcC
atoB
sdhB
sdhA
sdhD
sdhC

b

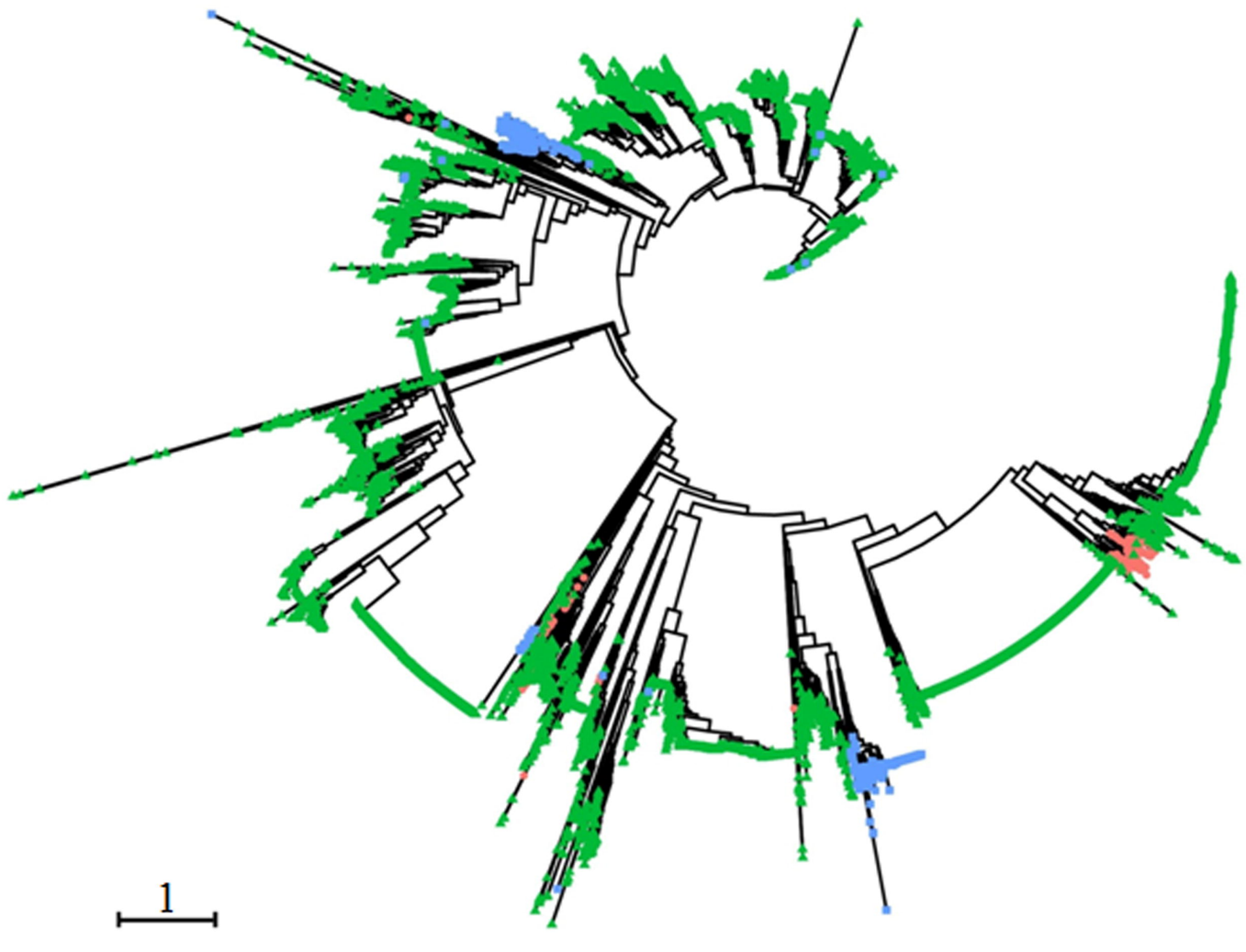
1